Korean J. Chem. Eng., **20**(5), 803-811 (2003)

Characteristics of Solitary Waves on a Running Film Down an Inclined Plane Under an Electrostatic Field

Hyo Kim†

Department of Chemical Engineering, University of Seoul, 90 Jeonnong-Dong, Dongdaemun-Gu, Seoul 130-743, Korea
(*Received 21 February 2003 • accepted 21 May 2003*)

Abstract−For the study on the nonlinear dynamics of thin-film flow running down an inclined plane under the effect of an electrostatic field, the mechanism of solitary waves has been examined by using a global bifurcation theory. First, the existence of solitary waves has been chased by using an orbit homoclinic to a fixed point of saddle-focus type in a linearized third-order ordinary differential equation which resulted from the evolution equation in a steady moving frame. Then, the trajectories with several kinds of solitary waves have also been searched numerically for the nonlinear system. In addition, the behavior of these waves has been directly confirmed by integrating the initial-value problem. The slightly perturbed waves at the inception eventually evolve downstream into almost permanent pulse-like solitary waves through the processes of coalescence and repulsion of the triggered subharmonics. In the global aspects the flow system at a given Reynolds number becomes more unstable and chaotic than when there is no electrostatic force applied.

Key words: Electrostatic Field, Solitary Waves, Global Bifurcation, Homoclinic, Saddle-Focus Type

INTRODUCTION

As a liquid layer flows down an inclined plane, it is susceptible to the development of instability to turbulence. The linear stability theories in parallel flows were first investigated by Benjamin [1957] and Yih [1963]. They identified the regimes of linear stability and determined the critical Reynolds number for instability. Then, the weakly nonlinear analysis as an extended work for the linear theory was performed by several authors, such as Benny [1966], Gjevik [1970], Lin [1974], and Chang [1989]. Lin [1974] conducted a weakly nonlinear analysis near the critical Reynolds number and found a transition value separating supercritical from subcritical regime. Chang [1989] examined the steady waves near the critical Reynolds number and discovered two sets of waves, i.e., one family of periodic waves and a single solitary wave by using a second-order bifurcation analysis of an interface equation.

The interaction dynamics between the thin film flow and an electrostatic field was studied for the first time by Kim et al. [1992] to answer the feasibility of a new design concept of a space radiator. In that article the basic question of how the liquid layer running down an inclined plane and an electrostatic field would interact with each other was answered. Kim [1997] extended this research scope to nonlinear stability to address two-dimensional surface wave evolution. The applied electrostatic field always made the flow system more unstable when compared with the free-charged case.

The aim of the present work is to explore the existence and interaction of solitary waves on a fluid layer running down an inclined plane under an electrostatic field. In the absence of the externally applied electrostatic force, i.e., in the fluid system drained purely under gravity, Pumir et al. [1983], Chang [1986, 1987], and Chang et al. [1993] systematically analyzed the nonlinear dynamics of surface waves moving down an inclined or a vertical plane. They studied and simulated numerically the mode of the solitary waves propagating downstream at constant speed without changing their shapes.

Beyond the linearly unstable inception region, there would be the evolution of short periodic and nearly sinusoidal waves, and then after this regime very long solitary waves occur and dominate downstream until breaking into non-stationary three-dimensional wave patterns.

Hence, these phenomena will easily be expected to happen in the flow mechanism affected by an electrostatic field while their instability behavior has different mode. First, the onset conditions of solitary waves and their characteristics in the proposed electrohydrodynamic system have been found here numerically by using the homoclinic orbits which are usually employed to track the aspects of global bifurcation and chaos [Chang et al., 1987]. Several types of solitary waves can be classified according to their number of humps. Next, using the solitary-wave onset values of Reynolds number and wave velocity resulting from the viewpoint of dynamical system theory, the initial-value evolution equation is integrated directly to examine the development of solitary waves through the process of a great deal of coalescence and repulsion between adjacent waves. The obtained target equation has been based on the long wave lubrication approximation at low Reynolds numbers, Re~O(1).

The subsequent sections are composed of evolution equation and linear stability, stationary solitary waves in a moving coordinate, numerical integration of the initial-value problem, and finally the results are concluded.

EVOLUTION EQUATION AND LINEAR STABILITY

The liquid layer is assumed an incompressible, viscous and electrically conductive thin film running down an inclined plane under the action of gravity g. Above the liquid layer there is a vacuum. Within the vacuum region at a distance H from the plane of length L locates a charged foil which has the same length as the plane. This

†To whom correspondence should be addressed.
E-mail: hkim@uos.ac.kr

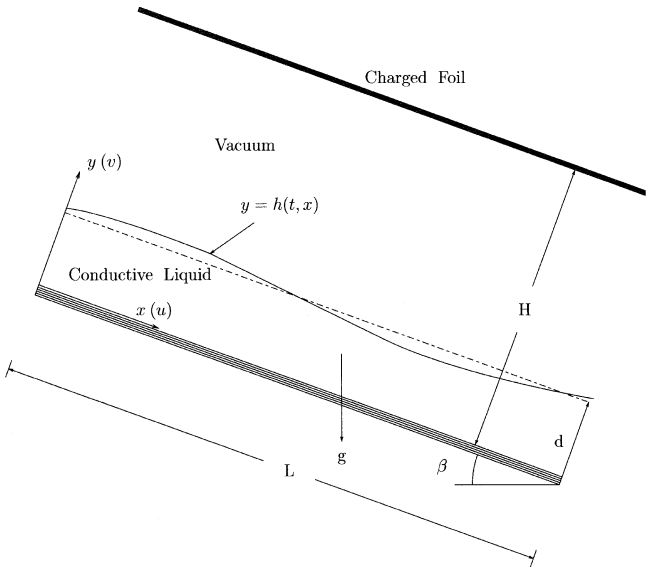

Fig. 1. The physical configuration of the plane flow under an electrostatic field.

situation is depicted in Fig. 1. An electrostatic field from the charged foil will interact with the liquid flow through the induced pulling-over force. Hence the film has been shown more unstable than that in a free-charged case [Kim et al., 1992; Kim, 1997]. Suppose that d is defined as the characteristic thickness of the primary film flow, then the parameter ξ=d/L will be very small if the film is thin, i.e., thin relative to the expected length scale of the disturbances in the horizontal.

Following the procedures already set up by Kim [1997], who interpreted the longwave instabilities of the thin layer as the result of the combined effects of electrostatic force, gravity and surface tension, the dimensionless evolution equation describing the behavior of the film thickness h(x, t) can be obtained by assuming the Reynolds number Re~O(1), the capillary number Ca~O(ξ^2) and the dimensionless electric force constant K~O(1). The result is given by

$$h_t+2h^2h_x+\xi\frac{\partial}{\partial x}\left(\frac{8}{15}\mathrm{Re}h^6h_x-\frac{2}{3}\mathrm{B}h^3h_x+\frac{2}{3}\frac{\xi^2}{\mathrm{Ca}}h^3h_{xxx}\right)+\frac{4}{3}\xi\mathrm{K}\frac{\partial}{\partial x}\left(\frac{\mathrm{H}^2}{(\mathrm{H}-h)^3}h^3h_x\right)=0, \tag{1}$$

where B is the cotangent of the angle β between the horizontal and x-axis. The subscripts represent the partial derivatives. The characteristic unit of flow velocity is employed as equal to the maximum velocity of the basic plane flow. The unit length in Eq. (1) is taken the depth d of the primary flow. Here the fluid is assumed a perfect conductor.

Next, to perform a linear stability analysis the Eq.(1) is perturbed about its steady-state solution, i.e., h(x, t)=1+$\bar{h}$(x, t). The small disturbance $\bar{h}$ is assumed to have a simple harmonic form, i.e., $\bar{h}$=exp {iα(x−ct)}, where $\alpha\geq 0$ is the wavenumber of the disturbance and c is the complex wave speed, i.e., $c=c_r+ic_i$. For positive α, if c_i is negative the flow is linearly stable, while if c_i is positive the flow becomes linearly unstable. Therefore in an α, Re diagram, the condition $c_i=0$ gives a neutral curve which defines the critical Reynolds number:

$$\mathrm{Re}_c=\frac{5}{4}\mathrm{B}+\frac{5}{4}\alpha^2\frac{\xi^2}{\mathrm{Ca}}-\frac{5}{2}\mathrm{K}\frac{\mathrm{H}^2}{(\mathrm{H}-1)^3}. \tag{2}$$

When K=0, Eq. (2) reduces to the same result studied by Gjevik [1970]. It can be seen that the first two terms in the right hand side of Eq. (2) act as stabilizing effects while the last one describes the instability.

SOLITARY WAVES IN A MOVING COORDINATE

Beyond a short transition region from the inlet of the flow, under some specific conditions the perturbed sinusoidal waves evolve downstream into distinct pulse-like solitary waves which travel steadily at constant speeds over a comparatively long distance. Unlike the sinusoidal waves, the solitary wave has a wide band of Fourier harmonics whose phases are locked. Due to its strong nonlinearity, it is hard to find out the constructing conditions of the solitary waves which will dominate all subsequent interfacial dynamics. Hence, to effectively track the evolving mechanism of pulse-like solitary waves in the proposed electrohydrodynamics, one can numerically set up the special solutions to Eq. (1) from the viewpoint of the dynamical systems theory. In a moving frame of z=x−vt, the waves are assumed to travel without deformation in the frame moving at a constant speed v relative to the laboratory frame. In terms of the moving coordinate, Eq. (1) will be governed by an ordinary differential equation, i.e., by letting h(x, t)=h(z) and denoting derivatives with respect to z by primes, Eq. (1) with ξ=1 can be transformed into the ordinary differential equation

$$-\frac{3}{2}\mathrm{v}h+h^3+\frac{4}{5}\left(\mathrm{Re}h^3-\frac{5}{4}\mathrm{B}+\frac{5}{2}\mathrm{K}\frac{\mathrm{H}^2}{(\mathrm{H}-h)^3}\right)h^3h'+\frac{1}{\mathrm{Ca}}h^3h'''=1-\frac{3}{2}\mathrm{v}. \tag{3}$$

To find out the above result, the Nusselt flat film condition at infinity has been applied: when z goes to ±∞, h tends to 1 and h'(z), h''(z), h'''(z) tend to zero.

Before numerically integrating Eq. (3) to find out the solutions associated with the pulse-like solitary waves, it is desirable to conduct a local analysis around the fixed (equilibrium or critical) points so as to confirm whether the solutions exist or not in advance. The dynamical behavior of the system linearized about the fixed points usually gives very significant information to predict the structural stability of the original nonlinear dynamic system. Depending on the types of the fixed points, the phase portrait is structurally stable or not. For instance, hyperbolic fixed points that will be hopefully sought in the present problem illustrate the important general notion of structural stability [Strogatz, 1998]. For this dynamical systems analysis, first Eq. (3) has to be written in the form of a first-order differential system:

$$\begin{aligned}U_1'&=U_2\\U_2'&=U_3\\U_3'&=\mathrm{Ca}\left[\frac{1-U_1}{U_1^3}\left(1+U_1+U_1^2-\frac{3}{2}\mathrm{v}\right)-\frac{4}{5}\left(\mathrm{Re}U_1^3-\frac{5}{4}\mathrm{B}+\frac{5}{2}\frac{\mathrm{K}H^2}{(\mathrm{H}-U_1)^3}\right)U_2\right],\end{aligned} \tag{4}$$

where U_1=h, U_2=h', U_3=h''. The system constitutes a flow in the

phase space made by (U_1, U_2, U_3) and thus a phase point traces out a solution of Eq. (4). For the nonlinear system like Eq. (4), there is typically no hope of finding the trajectories analytically because it is too complicated to provide much insight. Therefore to find the system's phase portrait qualitatively, it is necessary to figure out a phase portrait of the corresponding linear system near the fixed point. Fixed points of Eq. (4) are given by

$$U_2 = U_3 = 0,\ (1-U_1)\left(1+U_1+U_1^2-\frac{3}{2}v\right)=0. \tag{5}$$

There are two kinds of fixed points, that is, (U_1, U_2, U_3)=(h_1, 0, 0) or (U_1, U_2, U_3)=(h_2, 0, 0), where $h_1=1$ and $h_2(\neq 1)$ is the positive root of the equation $1+U_1+U_1^2-(3/2)v=0$. At the fixed point (1, 0, 0), the eigenvalues of the linearized system are solutions of the equation

$$\lambda^3+\frac{4}{5}Ca\left[Re-\frac{5}{4}B+\frac{5}{2}\frac{KH^2}{(H-1)^3}\right]\lambda-\frac{3}{2}Ca(v-2)=0. \tag{6}$$

It is clear that for $v>2$ and $Re>(5/4)B-(5/2)KH^2/(H-1)^3$, there are three eigenvalues λ_i(i=1, 2, 3) in Eq. (6) of which one (λ_1) is a positive real eigenvalue 2ρ and the others are $-\rho\pm i\omega$ (complex conjugate) with a negative real part. The fixed point hence is hyperbolic and the three eigenvalues construct a saddle-focus homoclinic orbit structure with a two-dimensional stable manifold and a one-dimensional unstable manifold. The solitary wave that is being sought now will be well defined by the homoclinic trajectories because it satisfies the Nusselt flat film condition at $z=\pm\infty$. When $v<2$, the situation will be opposite to the case of when $v>2$, that is, there are a one-dimensional stable manifold and a two-dimensional unstable manifold. The physical consequences will also have different modes around v=2. When $v>2$, the front part of a solitary pulse which corresponds to $z\rightarrow\infty$ shows damped oscillations because of the complex conjugate λ_2 and λ_3 with a negative real part while the rear smoothly gets down to 1 without any oscillation because z tends to $-\infty$ and λ_1 is a positive real. When $v<2$, the solitary wave mode is completely reversed and symmetric to the case of when $v>2$. Hence v=2 plays an important role of the border of the velocity perturbations in the nonlinear fluid dynamics producing solitary waves.

Considering the linearized system about the other fixed point (U_1, U_2, U_3)=(h_2, 0, 0), where h_2 is the positive root of $1+h+h^2-(3/2)v=0$ ($h_2>1$), the corresponding eigenvalues are solutions of the equation

$$\lambda^3+\frac{4}{5}Ca\left[Reh_2^3-\frac{5}{4}B+\frac{5}{2}\frac{KH^2}{(H-h_2)^3}\right]\lambda-\frac{3Ca}{2h_2^3}(v-2h_2^2)=0. \tag{7}$$

For $v>2$, h_2 is always greater than 1 and Eq. (7) constructs a two-dimensional unstable and a one-dimensional stable manifolds. In general the two-dimensional manifold will be connected to the two-dimensional stable manifold created by the other fixed point (U_1, U_2, U_3)=(1, 0, 0). The trajectory joining these two different fixed points is called heteroclinic [Wiggins, 1990]. The heteroclinic orbit is a solution describing a hydraulic jump with a height h_2 upstream and h_1(=1) downstream. This heteroclinic behavior is irrelevant to the present solitary wave dynamics and thus the homoclinic trajectory starting from (1, 0, 0) and coming back to the same point will be only considered to search for distinct pulse-like solitary waves in a global phase space.

1. Numerical Search for Solitary Waves

With a set of parameters Re, B, Ca, K and H fixed, the certain value of v producing a solitary wave has to be chased numerically by solving the ordinary differential system of Eq. (4) in a three-dimensional phase space centered at the fixed point (1, 0, 0). If the value of v is exactly right, the solution trajectory starting along the two-dimensional unstable manifold will come back to the neighborhood of the fixed point along the one-dimensional stable manifold. However, it is very complicate to find the specific v at one try because the system of Eq. (4) is so delicate that the solution on the unstable manifold would not most often return to the fixed point. Hence the exact value of v has to be found numerically by continuously adjusting the previously calculated value of v to approximate the homoclinic trajectory. From an initially assumed value of v the integration of system Eq. (4) supplies a phase portrait of solutions. If the trajectory is not homoclinic, the v has been changed to an improved value. The modification of the value v would last until the homoclinic trajectory maintains, that is, the distance between the returning trajectory and the fixed point is kept the minimum. The minimum distance means that it is not available to get an exact homoclinic trajectory but an approximate one. However, the present numerical approach confirms the existence of the distinct pulse-like solitary waves.

With Re=6, B=5, 1/Ca=3,000, K=10 and H=10 fixed, three kinds of homoclinic trajectories are obtained corresponding to different

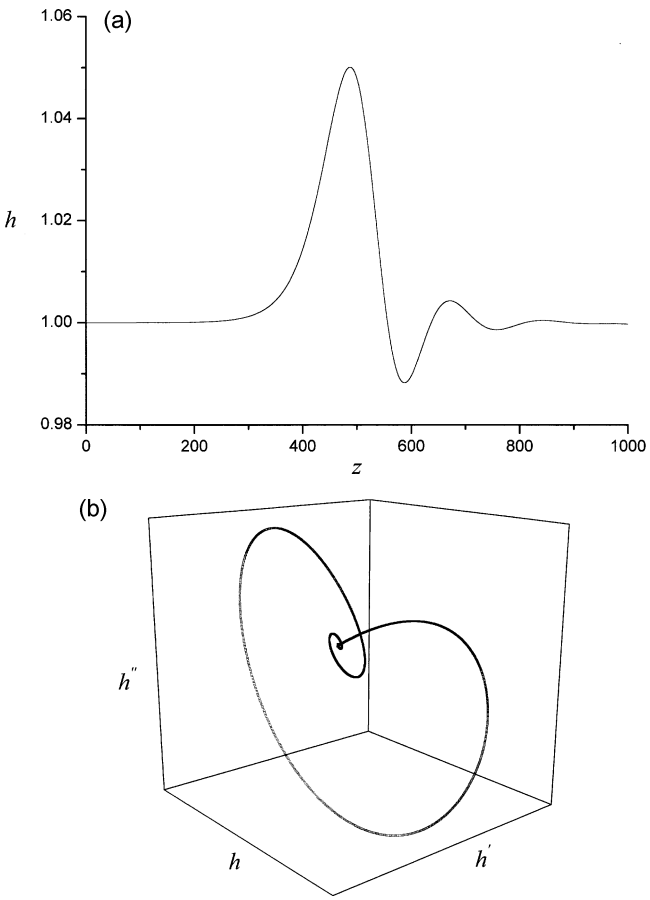

Fig. 2. (a) The single hump solitary wave at v=2.078553975 (Re=6, B=5, 1/Ca=3,000, K=10, H=10). (b) The saddle-focus homoclinic orbit for the single hump solitary wave at v=2.078553975 (Re=6, B=5, 1/Ca=3,000, K=10, H=10).

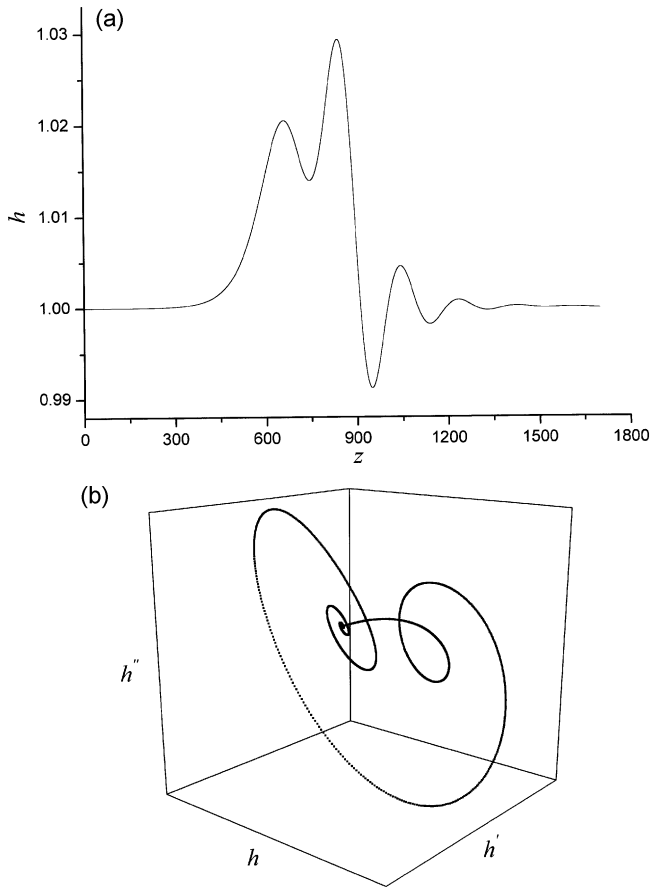

Fig. 3. (a) The double hump solitary wave at v=2.040491995 (Re=6, B=5, 1/Ca=3,000, K=10, H=10). (b) The saddle-focus homoclinic orbit for the double hump solitary wave at v=2.040491995 (Re=6, B=5, 1/Ca=3,000, K=10, H=10).

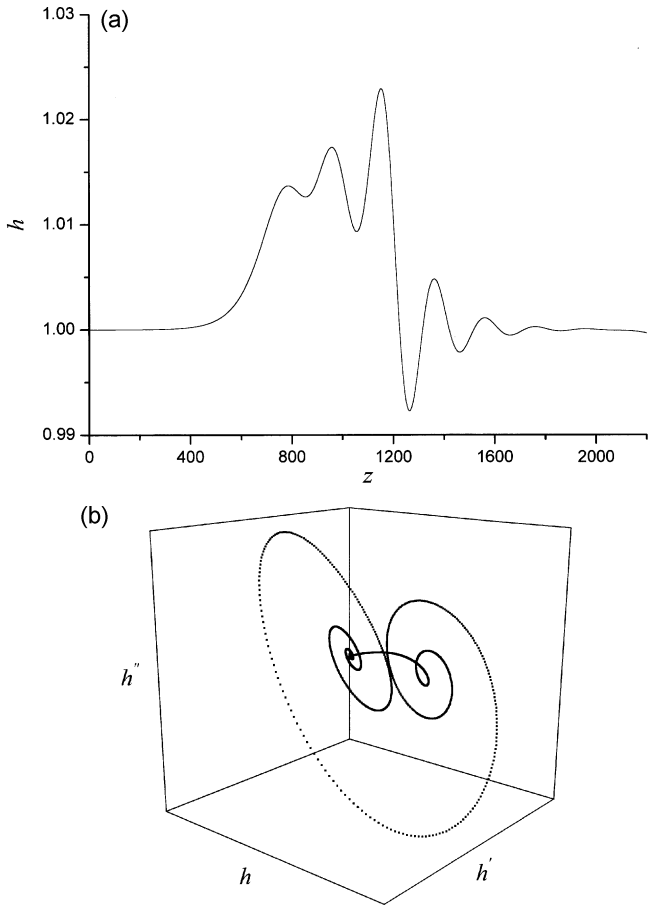

Fig. 4. (a) The triple hump solitary wave at v=2.030010035 (Re=6, B=5, 1/Ca=3,000, K=10, H=10). (b) The saddle-focus homoclinic orbit for the triple hump solitary wave at v=2.030010035 (Re=6, B=5, 1/Ca=3,000, K=10, H=10).

values of v. The different homoclinic trajectories are classified by the number of the principal humps in the solitary waves. Fig. 2a and Fig. 2b show the single hump solitary wave and the corresponding phase orbit, respectively, at the numerically obtained value of v=2.078553975. In Fig. 3(a, b) and Fig. 4(a, b), the double hump (v=2.040491995) and the triple hump (v=2.030010035) solitary waves and phase portraits are depicted respectively. All the solitary waves have a velocity greater than 2 and different values of v. Thus in a (Re, v) domain, the solitary waves will have different branches to the number of humps as seen in Fig. 5. All the solutions meet at the values of v=2 and $Re=5/4B-5/2[KH^2/(H-1)^3]$. It has been also found that there are maximumly attainable values of Re corresponding to the types of solitary waves, and as the number of humps is increased, the span of the velocities defining the specific kinds of solitary waves becomes larger. In addition, it has been observed that the amplitude and velocity of every solution on the upper branch of Fig. 5 are rapidly augmented as Re decreases. To check the effect of electrostatic force strength on the occurrence of solitary waves, the values of Re and v for a single hump solitary wave are plotted in Fig. 6 according to several values of K. It is worth noticing that at a constant velocity the Reynolds number creating the solitary wave becomes smaller as the electric force gets stronger, i.e., the film flow becomes more unstable in the nonlinear dynamics.

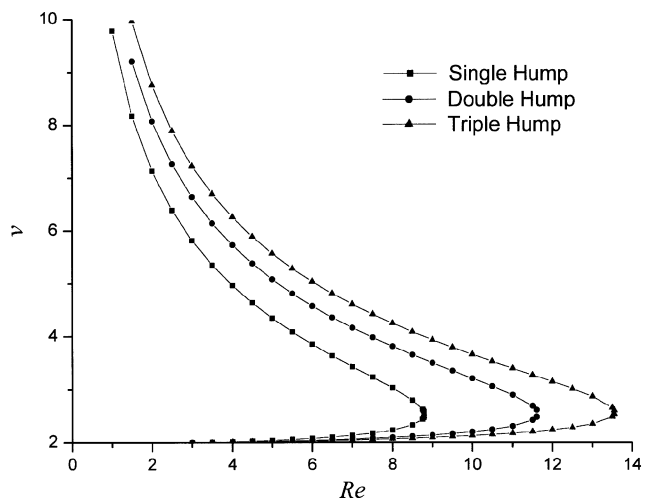

Fig. 5. Re versus v for the homoclinic orbits at B=5, 1/Ca=3,000, K=10 and H=10.

2. Analytical Approach for Some Limiting Cases

Investigating Fig. 5 around two ends of the curves, it can be easily expected there are some linearities in the solutions as v approaches to zero or infinity. In the vicinity of $\{v=2, Re=5/4B-5/2[KH^2/(H-1)^3]\}$, the numerical results show that the amplitude of solitary wave

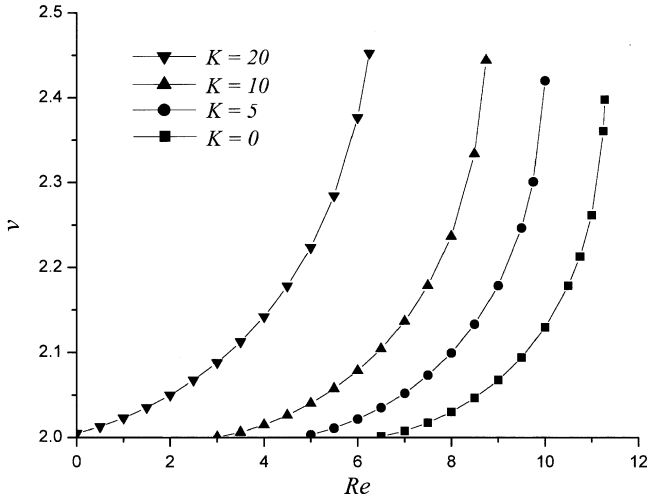

Fig. 6. Re versus v for single hump solitary waves with the K's at B=5, 1/Ca=3,000 and H=10.

h is very small if it is compared with the value obtained from the other locations. Hence to get an analytical approach to this domain, v and h are assumed such that $v=2(1+\varepsilon)$ and $h=1+\varepsilon\phi$(ε is very small parameter) to get the following differential equation from Eq. (3):

$$\phi''' + \mu\phi' + \phi(\phi-1) = 0, \tag{8}$$

where the dot now represents the new derivative of $\bar{z} = (3\varepsilon Ca)^{1/3} z$ and the constant μ is given by

$$\mu = \frac{4}{5}\left(\frac{Ca}{9}\right)^{1/3} (\varepsilon)^{-2/3}\left(Re - \frac{5}{4}B + \frac{5}{2}K\frac{H^2}{(H-1)^3}\right). \tag{9}$$

Since for all $\mu \geq 0$ Eq. (8) always has saddle-focus eigenvalues, there exist families of homoclinic trajectories if the following condition is satisfied:

$$v - 2 \sim \left(Re - \frac{5}{4}B + \frac{5}{2}K\frac{H^2}{(H-1)^3}\right)^{3/2}. \tag{10}$$

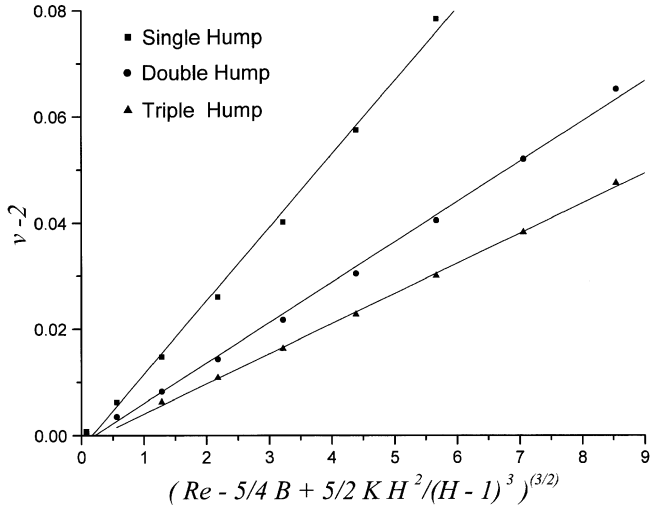

Fig. 7. v−2 versus $[Re-5/4B+5/2KH^2/(H-1)^3]^{3/2}$ for B=5, 1/Ca=3,000, K=10 and H=10.

To confirm the above analytic approach, the calculated values of (v−2) have been plotted to $[Re-(5/4)B+(5/2)K\{KH^2/(H-1)^3\}]^{3/2}$ for the three kinds of solitary waves in Fig. 7 which shows a good agreement with the asymptotic analysis around $\{v=2, Re=5/4B-5/2[KH^2/(H-1)^3]\}$.

To consider another analytical approach for the other limiting case, i.e., as $Re \to 0$ and $v \to \infty$, Eq. (3) has been modified such that

$$\frac{h-1}{h^3}\left(h^2+h+1-\frac{3}{2}v\right)+\left(\frac{4}{5}Reh^3-B+2K\frac{H^2}{(H-h)^3}\right)h' + \frac{1}{Ca}h''' = 0. \tag{11}$$

Integration of Eq. (11) over $(-\infty, \infty)$ yields

$$\int_{-\infty}^{\infty}\frac{h-1}{h^3}\left(h^2+h+1-\frac{3}{2}v\right)dz = 0, \tag{12}$$

where the assumption H>>h is used. Hence if h is replaced with h_{max}, the deduced result is obtained from the analysis of orders of magnitude:

$$v \sim h_{max}^2. \tag{13}$$

In addition, the integration after the multiplication of Eq. (11) by h' leads to

$$Re \sim h_{max}^{-3}. \tag{14}$$

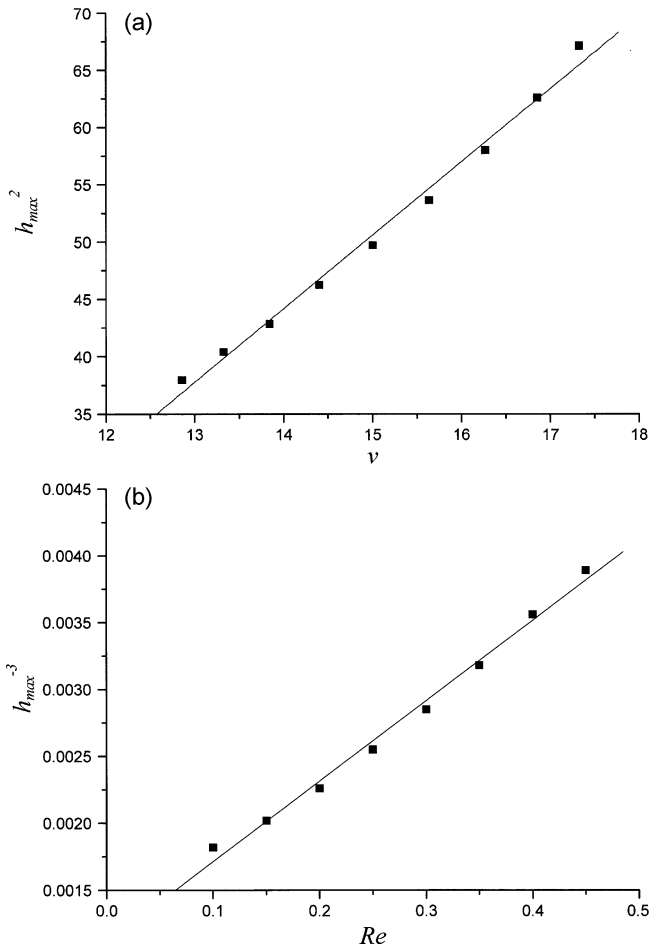

Fig. 8. (a) v versus h_{max}^2 for B=5, 1/Ca=3,000, K=10 and H=10. (b) Re versus h_{max}^{-3} for B=5, 1/Ca=3,000, K=10 and H=10.

The asymptotic behaviors of Eq. (13) and Eq. (14) are in good agreement with the numerical calculations as shown in Fig. 8a and Fig. 8b, respectively.

The analytical approach for the limiting cases is similar to that done by Pumir et al. [1983] who considered the behavior of solitary waves for the thin film flow without the electrostatic field.

NUMERICAL INTEGRATION OF THE INITIAL-VALUE PROBLEM

In the previous section, the existence of solitary waves has been pursued numerically in a steady moving coordinate. However, the real evolution situation is time dependent and thus it is necessary to confirm the formation of pulse-like solitary waves that will dominate all subsequent interfacial dynamics. For this demonstration the initial value problem given by Eq. (1) has been integrated with periodic boundary conditions. The periodic computational domain is defined in $-\pi \le \alpha x \le \pi$ (α is a wavenumber) for the laterally unbounded flow region. With ξ=0.02, α=0.1, Re=6, B=5, 1/Ca=3,000, K=10 and H=10 fixed, the time marching of Eq. (1) is performed by virtue of a fourth-order modified Hamming's predictor-corrector method with the maximum tolerance of 10^{-11} in the centered finite difference space scheme. For the initial forcing condition the flat film is slightly perturbed as a small cosine-bell bump at x=0 with the maximum amplitude of 1.02 as shown in the first graph (t=0) of Fig. 9(a). In this case since the value of Re_c is 2.836, if Re is less than Re_c, the flow becomes stable, i.e., the amplitude of the film tends to the basic one h=1 at large times. For $Re > Re_c$ the interfacial height h which is initially perturbed grows and buckles to evolve into solitary pulses. If the Reynolds number is too much greater than the critical one, the perturbed wave front becomes steeper and at last the flow system turns into a catastrophic situation as studied by Kim [1997] who calculated the nonlinear film evolution with various wavenumbers and obtained the free-surface growth rates using the Fourier-spectral method.

It will be demonstrated that the growth of the initial localized perturbation and the interaction of the triggered subsequent ripples cause the free surface to coalesce into a bigger solitary pulse which dominates the interfacial dynamics. The running film under the electrostatic field with the infinitesimal disturbance as shown at t=0 in Fig. 9(a) has been excited downstream through the interaction of the emerging wavetrains after the exponential growth of the free surface from the inceptive stage. At t=300 in Fig. 9(a) the advent of a big solitary-like wave is observed among the small wavetrains through a complicated nonlinear selection mechanism. As time further elapses, the other graphs in Fig. 9(a) represent the active development and propagation of waves conceiving solitary pulses through the coalescence of neighboring ripples. Throughout the graphs in Fig. 9(b) it can be easily seen that most of the ripples appeared in Fig. 9(a) are merging into big significant humps which will be evolved into solitary waves later through the processes of attracting and repelling with each other. In this time range the shapes of the interface are

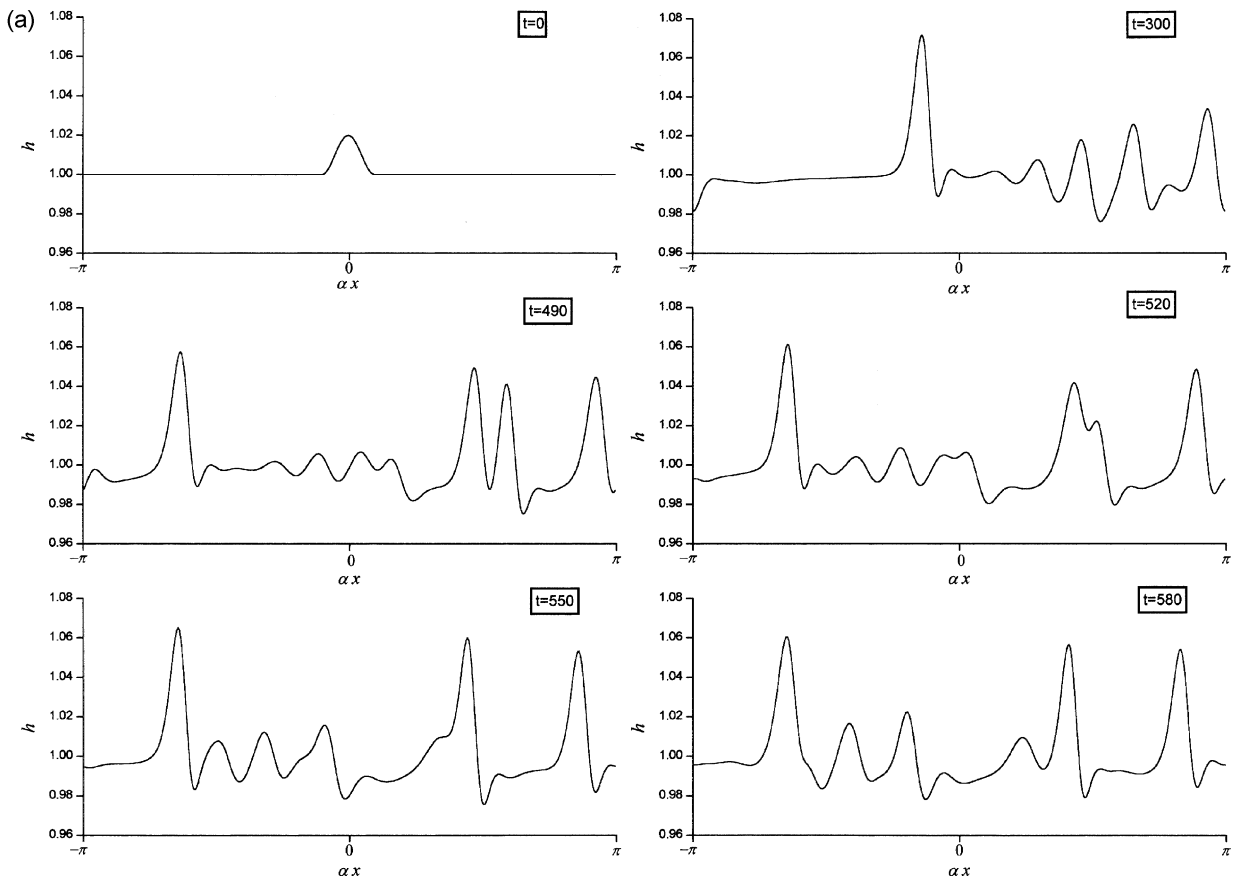

Fig. 9. (a) Surface-wave behavior of Eq. (1) for 0≤t≤580 at ξ=0.02, α=0.1, Re=6, B=5, 1/Ca=3,000, K=10, and H=10.

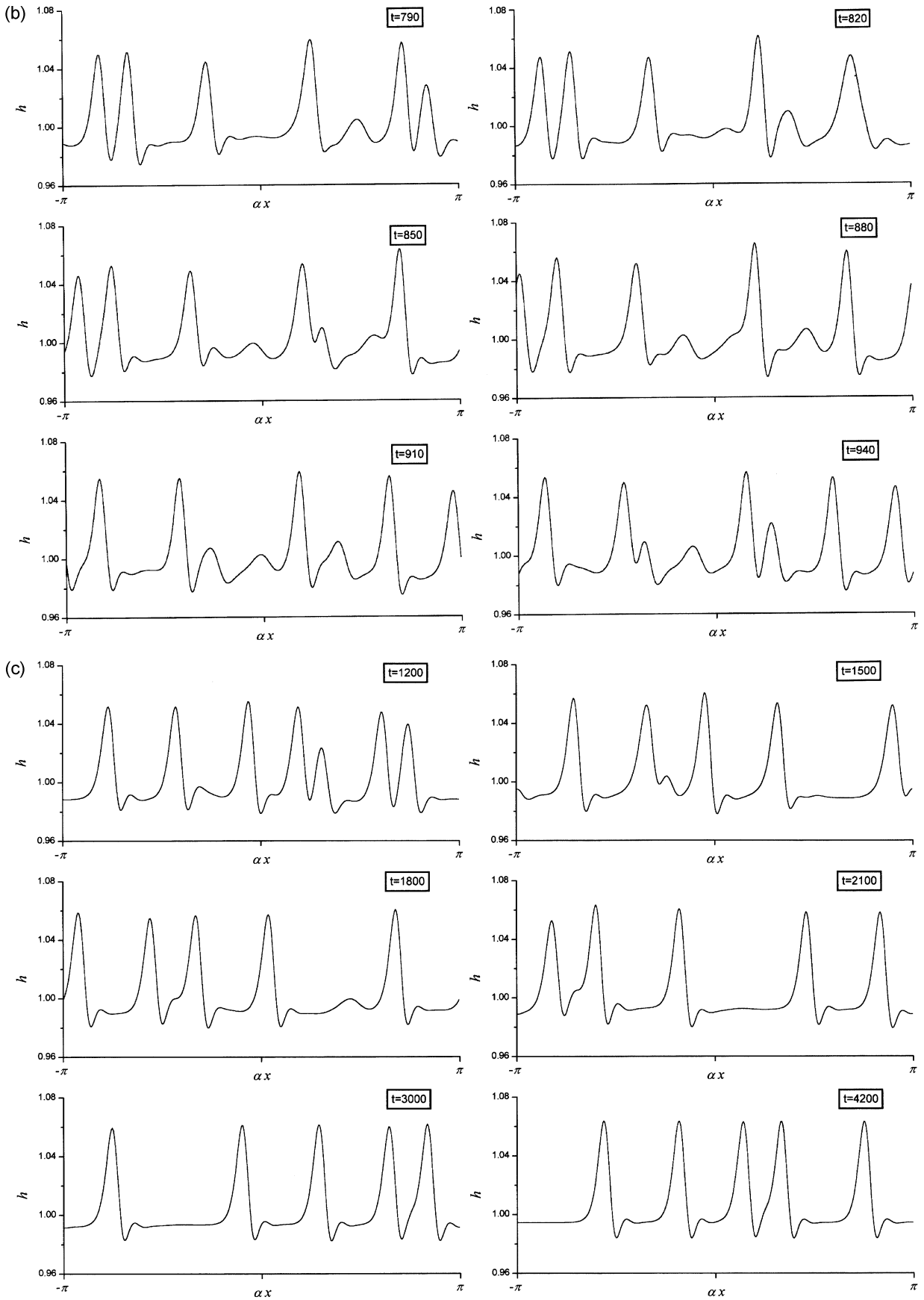

Fig. 9. (b) Surface-wave behavior of Eq. (1) for 790≤t≤940 at ξ=0.02, α=0.1, Re=6, B=5, 1/Ca=3,000, K=10, and H=10. (c) Surface-wave behavior of Eq. (1) for 1,200≤t≤4,200 at ξ=0.02, α=0.1, Re=6, B=5, 1/Ca=3,000, K=10, and H=10.

still irregular with space and time changes. In Fig. 9(c) amazingly the solution tends toward a regular arrangement of pulse-like solitary waves after a very long time has passed. Until t=1,500, there is an active collision between big waves and small wave because the small-amplitude one is slower than the other big ones. At t=1,800 or t= 2,100 it is observed that the layer interface is almost all matured with the solitary waves while it is still affected by a small wave, which will be finally merged and disappeared as seen the graphs at t=3,000 or t=4,200 in Fig. 9(c). It is noticeable that as the solitary waves have formed, the thickness of the substrate layer has been considerably reduced comparing to the initial film depth. On the state of the thicker film at onset the gravity-capillary dispersion mechanism has delayed the phase locking of the Fourier modes to build up solitary waves. However once formed, the pulse-like solitary waves are less susceptible to transverse disturbances. If there is no more transverse secondary instability occurred to the layer, the solitary waves will dominate the electrohydrodynamics described by Eq. (1). The numerical simulations presented here undoubtedly confirmed that there exist solitary waves of the kind derived from the viewpoint of the dynamical systems theory.

CONCLUSIONS

The nonlinear dynamics composed of an evoultion equation describing thin-film flow running down an inclined plane under the effect of an electrostatic field has been closely examined for the mechanism of solitary waves. First of all, the existence of solitary waves has been searched by using an orbit homoclinic to a fixed point of saddle-focus type in a linearized third-order ordinary differential equation which resulted from the evolution equation in a moving frame at a constant speed v relative to the laboratory frame. Then, the trajectories with several kinds of solitary waves have been searched numerically for the transformed nonlinear system. Finally, to understand the nonlinear development of instability and transition to the pulse-like solitary waves, the initial-value problem given by the partial differential Eq. (1) has been integrated using periodic boundary conditions. The slightly perturbed sinusoidal wave at the inception is exponentially amplified downstream due to the linear instability mode. After this stage the convectively unsatble system is controlled by weakly nonlinear effects as the exponentially excited waves converge to the values of finite amplitiudes. The system is still unstable and thus the neighboring waves interact with each other to become a larger one due to a subharmonic instability. This kind of grown wave acts as a solitary wave whose phase is locked and eventurally dominates the interfacial dynamics if the Reynolds number $Re(>Re_c)$ is smaller than a certain value above which the interface becomes catastrophic. It has been numerically observed that in the nonlinear dynamics as well as in the linear one, the flow system at a given Reynolds number is more unstable and chaotic than there is no electrostatic force applied. In addition, as the electric force gets stronger the Reynolds number creating the solitary wave becomes smaller at a constant velocity, i.e, the film flow becomes more unstable in the nonlinear dynamics.

ACKNOWLEDGMENT

This study was supported by the grant from the University of Seoul in 2002 and the author gratefully acknowledges it.

NOMENCLATURE

B : $\cot\beta$
Ca : capillary number
c : complex wave speed
d : characteristic film thickness
g : gravity
H : dimensionless distance from plane to charged foil
h : dimensionless free-surface thickness
h_1, h_2 : solutions of U_1 in Eq. (5)
K : dimensionless electric force constant
L : characteristic length scale parallel to plane
Re : Reynolds number
t : dimensionless time
U_1 : h
U_2 : h'
U_3 : h''
v : dimensionless wave velocity
x : dimensionless distance coordinate parallel to plane
y : dimensionless distance coordinate perpendicular to plane
z : x − vt
$\bar{z}$: $(3\varepsilon Ca)^{1/3}z$

Greek Letters

α : wavenumber
β : inclination angle of plane with the horizontal
ε : small parameter
λ : eigenvalue
μ : dimensionless constant defined by Eq. (9)
ξ : d/L
ϕ : disturbed film thickness

Superscripts

' : derivative with z
• : derivative with $\bar{z}$
− : small disturbance

Subscripts

c : critical value
i : imaginary part
max : maximum value
r : real part
t : partial derivative with t
x : partial derivative with x

REFERENCES

Benjamin, T. B., "Wave Formation in Laminar Flow Down an Inclined Plane," *J. Fluid Mech.*, **2**, 554 (1957).
Benney, D. J., "Long Waves on Liquid Films," *J. Math. Phys.*, **45**, 150 (1966).
Chang, H.-C., "Evolution of Nonlinear Waves on Vertically Falling Films - a Normal Form Analysis," *Chem. Engrg. Sci.*, **42**, 515 (1987).
Chang, H.-C., "Onset of Nonlinear Waves on Falling Films," *Phys. Fluids A*, **1**, 1314 (1989).

Chang, H.-C., "Traveling Waves in Fluid Interfaces: Normal Form Analysis of the Kuramoto-Sivashinsky Equation," *Phys. Fluids*, **29**, 3142 (1986).

Chang, H.-C., Demekhin, E. A. and Kopelevich, D. I., "Nonlinear Evolution of Waves on a Falling Film," *J. Fluid Mech.*, **250**, 433 (1993).

Chang, K. S. and Aris, R., "Nonlinear Dynamics and Strange Attractors," *Korean J. Chem. Eng.*, **4**(2), 95 (1987).

Gjevik, B., "Occurrence of Finite-Amplitude Surface Waves on Falling Liquid Films," *Phys. Fluids*, **13**, 1918 (1970).

Kim, H., Bankoff, S. G. and Miksis, M. J., "The Effect of An Electrostatic Field on Film Flow Down an Inclined Plane," *Phys. Fluids A*, **4**, 2117 (1992).

Kim, H., "Long-Wave Instabilities of Film Flow under an Electrostatic Field : Two-Dimensional Disturbance Theory," *Korean J. Chem. Eng.*, **14**(1), 41 (1997).

Lin, S. P., "Finite Amplitude Side-Band Stability of a Viscous Film," *J. Fluid Mech.*, **63**, 417 (1974).

Pumir, A., Manneville, P. and Pomeau, Y., "On Solitary Waves Running Down an Inclined Plane," *J. Fluid Mech.*, **135**, 27 (1983).

Strogatz, S. H., "Nonlinear Dynamics and Chaos," 9th ed., Perseus Books, Massachusetts (1998).

Wiggins, S., "Introduction to Applied Nonlinear Dynamical Systems and Chaos," Springer-Verlag, New York (1990).

Yih, C.-S., "Stability of Liquid Flow down an Inclined Plane," *Phys. Fluids*, **5**, 321 (1963).